Simulation of soil water dynamics for uncropped ridges and furrows under irrigation conditions

Yongyong Zhang[1,2,3,4], Pute Wu[1,3,4,5], Xining Zhao[1,3,4], and Zikui Wang[3,4]

[1]Institute of Soil and Water Conservation, Chinese Academy of Sciences and Ministry of Water Resources, Yangling, Shaanxi Province 712100, China; [2]Graduate School of Chinese Academy of Sciences, Beijing 100049, China; [3]Institute of Water Saving Agriculture in Arid regions of China, Northwest A & F University, Yangling, Shaanxi Province 712100, China; and [4]National Engineering Research Center for Water Saving Irrigation at Yangling, Yangling, Shaanxi Province 712100, China.
Received 4 August 2011, accepted 11 October 2012.

Zhang, Y., Wu, P., Zhao, X. and Wang, Z. 2013. **Simulation of soil water dynamics for uncropped ridges and furrows under irrigation conditions**. Can. J. Soil Sci. **93**: 85–98. The ridge-furrow planting system combined with furrow irrigation can effectively increase soil moisture storage and improve water use efficiency in the semi-arid region of China. The precise soil water dynamics in ridge-furrow systems must be known in order to properly design ridge-furrow geometry and improve irrigation uniformity while reducing deep water percolation. The objective of this study was to investigate soil water distribution in the cross-sectional ridge-furrow infiltration, through laboratory experiments and numerical simulations. Six experimental treatments with three soil types (silty clay loam, silt loam, and sandy loam) were tested to monitor both soil water movement and cumulative infiltration in rectangular soil chambers. The HYDRUS-2D model was calibrated and experimentally validated to simulate soil water dynamics. The root mean square error (RMSE) and coefficient of determination (R^2) provide a satisfactory quantitative comparison of the goodness-of-fit between observed and simulated cumulative infiltration. The optimized parameters were accurate and the observed and simulated values were very close, which demonstrated HYDRUS-2D as a reliable tool for accurately simulating soil water movement and applied water volume in ridge-furrow irrigation system. In finer soil, the wetted vertical and horizontal distances were equal and soil water distribution was more uniform than that in coarser soil. A high potential of deep water percolation was produced in sandy loam soil. Cumulative infiltration decreased with the increase of initial soil water content, whereas the volume of wetted soil increased with the increase of initial soil water content. Narrow furrows for crops with deep rooting depth and wide furrows for crops with shallow rooting depth were selected in irrigation design. The 40 cm furrow size and higher furrow water depth (water level) were recommended in a ridge-furrow irrigation system.

Key words: Ridge-furrow, soil water dynamics, irrigation, HYDRUS-2D

Zhang, Y., Wu, P., Zhao, X. et Wang, Z. 2013. **Simulation de la dynamique de l'eau du sol sur les billons et dans les sillons non cultivés lorsqu'il y a irrigation**. Can. J. Soil Sci. **93**: 85–98. La culture sur billons et l'irrigation par sillon peuvent rehausser efficacement le stockage de l'eau dans le sol et permettre un meilleur usage de l'eau dans les régions semi-arides de la Chine. Pour tracer correctement la géométrie des billons et des sillons, et rendre l'irrigation plus uniforme tout en réduisant la percolation de l'eau en profondeur, il faut néanmoins connaître avec précision la dynamique de l'eau dans de telles configurations. L'étude devait examiner la distribution de l'eau par infiltration transversale des billons-sillons grâce à des expériences en laboratoire et à des simulations numériques. Les auteurs ont testé six traitements expérimentaux sur trois types de sol (loam argileux limoneux, loam limoneux et loam sablonneux) afin d'établir à la fois le déplacement de l'eau dans le sol et son infiltration cumulative dans des cellules rectangulaires de sol. Le modèle HYDRUS-2D a été étalonné et validé expérimentalement de manière à simuler la dynamique de l'eau dans le sol. L'écart-type (E.-T.) et le coefficient de détermination (R^2) permettent une comparaison quantitative satisfaisante de la qualité de l'ajustement entre l'infiltration qu'on observe et celle qui est simulée. Les paramètres optimisés sont exacts et les valeurs correspondent bien entre les observations et la simulation, signe que le modèle HYDRUS-2D est un outil fiable et reproduit avec précision le déplacement de l'eau dans le sol ainsi que le volume d'eau appliqué dans un système d'irrigation par sillon. Dans les sols à texture fine, la distance mouillée est identique verticalement et horizontalement, et l'eau est distribuée de manière plus uniforme que dans les sols à texture plus grossière. Le loam sablonneux présente un potentiel élevé de percolation en profondeur. L'infiltration cumulative diminue avec l'augmentation de la teneur en eau initiale du sol, le volume de sol humide augmentant avec la hausse de la teneur en eau initiale. Au niveau de l'irrigation, on a retenu des sillons étroits pour les cultures s'enracinant profondément et des sillons larges pour celles dont les racines étaient superficielles. On recommande des sillons de 40 cm et une plus grande quantité d'eau dans les sillons (niveau) pour les systèmes d'irrigation par sillon.

Mots clés: Sillon-billon, dynamique de l'eau du sol, irrigation, HYDRUS-2D

[5]Corresponding author (e-mail: gjzwpt@vip.sina.com, zhangxyz23@126.com).

Water scarcity in the semi-arid region of China is a critical problem for agricultural production. The ridge-furrow planting method, which is built by shaping the soil surface with alternate ridges and furrows along the contour, is introduced to improve soil moisture storage and effectively increase crop production in this area (Li and Gong 2002; Li et al. 2007). Implementing furrow irrigation in the ridge-furrow planting system is an effective way to supply water to crops and deal with the water shortage problem in an agricultural field in the region (Li and Gong 2002; Liu et al. 2010). Lateral infiltrated water volume must meet the needs of the plants grown on the ridges of soil or raised beds. Improper furrow irrigation design in field has some disadvantages such as higher deep water percolation, lower irrigation uniformity, and lower water use efficiency (Moravejalahkami et al. 2009); whereas optimally designed ridge-furrow geometry and uniform soil water distribution in the ridge-furrow planting system should produce higher soil moisture storage and overall water use efficiency. Therefore, research on soil water dynamics in the ridge-furrow configuration is needed.

The soil surface of the furrow bed is an interface that partitions surface water flow and subsurface infiltration during irrigation process (Abbasi et al. 2003a, b). Subsurface water flow is one of many critical and complex processes to control runoff, infiltration, and irrigation uniformity, which is taken into consideration for ridges/furrows width ratio design and irrigation system optimization (Liu and Lu 1989; Li et al. 2003). In furrow irrigation, parameters including cumulative infiltration, wetting pattern, and soil water distribution were monitored to investigate soil water dynamics (Sterlkoff and Sousa 1984; Izadi and Wallender 1985; Trout 1992; Abbasi et al. 2003a, b). Wetted perimeter, ridge width, and adjacent furrow number affected the cumulative infiltration as a function of time curve in field experiments (Liu and Lu 1989; Sun et al. 1994). Zhang et al. (2005) reported that hydraulic conductivity in the furrow bottom (surface seal) had the strongest influence on infiltration process compared with the other factors. The migration distances of wetting front and soil water movement in furrow irrigation were investigated in simulation experiments (Nie et al. 2009a, b).

Many water infiltration models have been developed to simulate subsurface water flow in furrow irrigation. On the one hand, analytical models such as the Philip model and empirical models usually quantify the applied water volume (Esfandiari and Maheshwari 1997; Moravejalahkami et al. 2009). Either the Philip equation or modified Kostiakov equation combined with wetted perimeter simulated cumulative infiltration very well over time (Liu and Lu 1989). Holzapfel et al. (2004) showed that infiltration in furrow irrigation can be represented by the Kostiakov and Kostialov–Lewis models. On the other hand, subsurface water flow in furrow irrigation was analyzed theoretically by a number of physically based models. Richards' equation is a classic model that has been successfully used to simulate variably saturated flow (Richards 1931). Many soil infiltration models were established based on Richards' partial differential equation in a variably saturated, rigid, isotropic porous soil medium (Abbasi et al. 2004; Mailhol et al. 2007; Crevoisier et al. 2008). A complete hydrodynamic furrow irrigation model (TRIDISUL) with two-dimensional Richards' equation was applied to simulate blocked furrow irrigation (Tabuada et al. 1995). Several Windows-based computer software packages are often used to simulate subsurface water flow based on Richards' equation, such as CHAIN-2D/3D (Wang et al. 1997), SWMS-2D/3D (Nie et al. 2009a; Yao et al. 2010), and HYDRUS-2D/3D (Abbasi et al. 2004; Mailhol et al. 2007). HYDRUS-2D (Šimůnek et al. 2006) is a well-known Microsoft Windows-based computer software package that is used for simulating water, heat, and/or solute transport in a two-dimensional variably-saturated porous medium. The Levenberg-Marquardt optimization algorithm is used to inversely estimate the soil hydraulic and/or solute transport parameters. The governing equation is numerically solved using Galerkin-type linear finite elements. A number of laboratory and field irrigation studies have been successfully utilized the HYDRUS-2D simulation model (Abbasi et al. 2004; Skaggs et al. 2004; Kandelous and Šimůnek 2010; Ebrahimian et al. 2011). The HYDRUS-2D model has also been used to simulate solute transport (e.g., bromine and nitrogen) and assess the effect of irrigation schedule, design, and management practices on nitrogen leaching (Abbasi et al. 2004; Mailhol et al. 2007; Crevoisier et al. 2008; Ebrahimian et al. 2011). The HYDRUS-2D model, as an available research and design tool, is useful for assessing the risks of nitrate leaching by selecting better irrigation and fertilization management practices. The simulation method has certain advantages over conventional field experiments, such as reduced cost and time. Furthermore, understanding variables affecting soil water distribution through models is needed for optimized design and better management of the ridge-furrow irrigation system.

In this study, we investigated soil water dynamics by simulation experiments, which avoided the added complexity caused by vegetation and additional site-specific factors. The objectives of this research were: (1) to use the experimental data (cumulative infiltration volume, wetting distance, and soil water distribution) to validate the HYDRUS-2D simulations in the cross-sectional uncropped ridge-furrow configuration under irrigated condition; and (2) to analyze the effect of soil physical properties and variables (furrow size and water depth) on applied water volume and soil water distribution using the HYDRUS-2D model. These results would provide guidance for the efficient design of ridge-furrow planting systems.

Table 1. Soil physical properties in the experiment

Soil texture classification	Soil particle size distribution (%)			Bulk density (g cm^{-3})
	Sand (0.05–2.00 mm)	Silt (0.002–0.05 mm)	Clay (<0.002 mm)	
Silty clay loam	8.2	61.9	29.9	1.4
Silt loam	35.8	50.4	13.8	1.45
Sandy loam	71.8	21.4	6.8	1.3

MATERIALS AND METHODS

Laboratory Experiment

Investigation of water infiltration using laboratory soil chamber in ridge-furrow irrigation was used to verify the utility of HYDRUS-2D simulations of soil water distribution. Three soils (sandy loam soil, silt loam soil, and silty clay loam soil; Canadian/USDA system) from the Loess Plateau, China, were collected from the 10- to 30-cm depth in fallow fields. Soil textural fractions were analyzed using the Laser Mastersizer 2000 (Malvern Instruments, Malvern, England). Bulk density was determined by manually by inserting a 50-mm by 50-mm ring soil sampler into a soil profile wall. The physical properties of the soils in the fields are summarized in Table 1.

The experimental setup consisted of a rectangular soil chamber and water supply system (a Mariotte flask) (Fig. 1). The rectangular soil chamber, made from 10-mm-thick plexiglass material, was 120 cm long (AD section), 20 cm wide (AE section) and 90 cm high (AB section). An inlet-pipe with an 8-mm-diameter rubber hole was installed at the ABCD section profile at a depth of 10 cm below the soil chamber surface and in the middle of the horizontal section (AD section). The bottom of the soil chamber (BCGF section profile) included many 2-mm parallel air vents for ventilation. One side of the soil chamber (EFGH section profile) contained a uniform distribution of side holes (20 mm) for measurement of soil water contents. Rubber stoppers were placed in the holes to prevent the soil from falling out of the soil chamber. The soil wetting pattern was inscribed on the plexiglass surface with a marker on two selected vertical surfaces of soil chamber (ABCD and EFGH section profiles) to validate the experimental accuracy. The Mariotte flask with a flexible hose was connected to an 8-mm-diameter rubber hole on the soil chamber to supply water. This system can maintain a constant hydraulic head under the irrigation furrow bed. The target variables affecting the infiltration process were tested in the rectangular soil chamber, and the shape of soil chamber had a negligible impact on the water flow pattern (Li et al. 2003; Zhang et al. 2005; Nie et al. 2009a, b).

The soils were collected and immediately air-dried at ambient temperature (15°C). The soil was passed through a 2-mm sieve before being packed into the experimental soil chamber (Fig. 1). Before packing, the soil was watered until the intended initial soil water content (Table 2) was reached. The prepared soil was

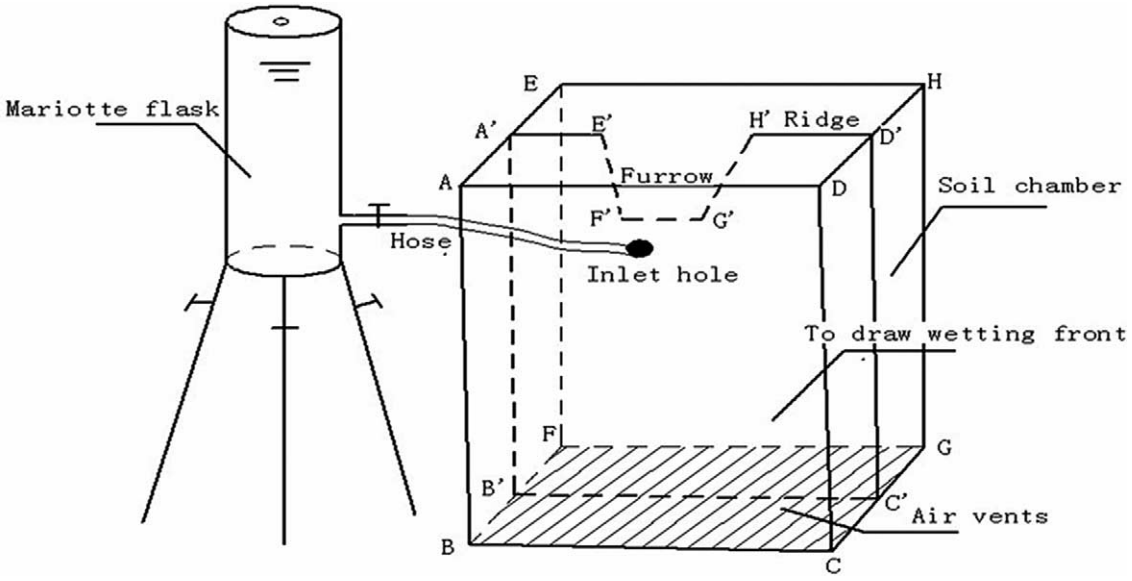

Fig. 1. Schematic representation of experimental setup for cross-sectional ridge-furrow infiltration.

Table 2. Summary of the designed variables for six experimental treatments

Exp. no.	Soil texture	Initial soil moisture ($cm^3\ cm^{-3}$)	Furrow size (cm)	Bulk density ($g\ cm^{-3}$)	Furrow water depth (cm)	Infiltration time (min)
1	Silty clay loam	0.096	20	1.45	7	150
2	Silty clay loam	0.055	60	1.4	9.7	150
3	Silt loam	0.068	40	1.45	10	150
4	Silt loam	0.110	60	1.5	10	90
5	Sandy loam	0.083	60	1.25	10	90
6	Sandy loam	0.054	40	1.35	9	150

loaded and compacted into the soil chamber in 5-cm increments to obtain the required bulk density (Table 2) and homogeneous soil profile. The packed soil in the entire chamber was allowed to equilibrate for 24 h to obtain a uniform distribution of water. To maintain zero evaporation, the soil was covered with a polyethylene sheet throughout the experimental process.

To examine the effect of soil texture, initial soil water content, and furrow size on ridge-furrow irrigation infiltration, six experimental treatments with two replications were conducted in the soil chamber (Table 2). The target variables were designed according to real field values. The packed soil was excavated into a ridge-furrow configuration (Fig. 1). The specified furrow size was designed according to Table 2. The furrow had a height of 15 cm and a slope coefficient of 1.73. The furrow water depth is the standing water height from the bottom of a furrow, and the furrow water depth was maintained at 10 cm (Abbasi et al. 2003a) with minor fluctuations (Table 2). The furrow water depth was maintained by adjusting the Mariotte flask before the beginning of the tests. Each experiment lasted for 90 to 150 min to ensure a free-drainage bottom boundary. During each experiment, the positions of the moving wetting front in vertical and horizontal directions on two selected vertical surfaces of soil chamber (ABCD and EFGH section profile) were recorded with a marker every 20 min. The cumulative infiltration volume was recorded by taking readings of the graduated Mariotte flask every 5 min. As the experiment ended, the soil was immediately sampled at different positions of the ridge, ridge shoulder, and furrow using a 2-cm-diameter soil auger. The sampled soil was oven dried at 105°C for 8 h to determine the gravimetric soil water content. The volumetric soil moisture was calculated by multiplying the gravimetric water content by bulk density.

Numerical Simulation

Subsurface Water Flow Model

Water infiltration and redistribution in the cross-sectional ridge-furrow configuration is assumed to be a two-dimensional isothermal Darcian water flow in a variably saturated rigid porous medium (Tabuada et al. 1995; Abbasi et al. 2004; Mailhol et al. 2007; Crevoisier et al. 2008; Nie et al. 2009a). The governing equation for subsurface water flow was described by Richards' equation (1931) in its two-dimensional form.

$$\frac{\partial\theta}{\partial t}=\frac{\partial}{\partial x}(K(h)\frac{\partial h}{\partial x})+\frac{\partial}{\partial z}(K(h)\frac{\partial h}{\partial z})+\frac{\partial K(h)}{\partial z} \quad (1)$$

where θ is volumetric water content ($cm^3\ cm^{-3}$), h is soil water pressure head (cm), t is time (min), $K(h)$ is unsaturated hydraulic conductivity ($cm\ min^{-1}$), x is horizontal space coordinate (cm), and z is the vertical space coordinate (cm).

The unsaturated hydraulic conductivity function, $K(h)$, was described using the capillary model of Mualem (1976). The soil water retention curve, $\theta(h)$, was described using the closed-form equation of van Genuchten (1980) as follows.

$$K(h)=K_sS_e^l[1-(1-S_e^{\frac{1}{m}})^m]^2 \quad (2)$$

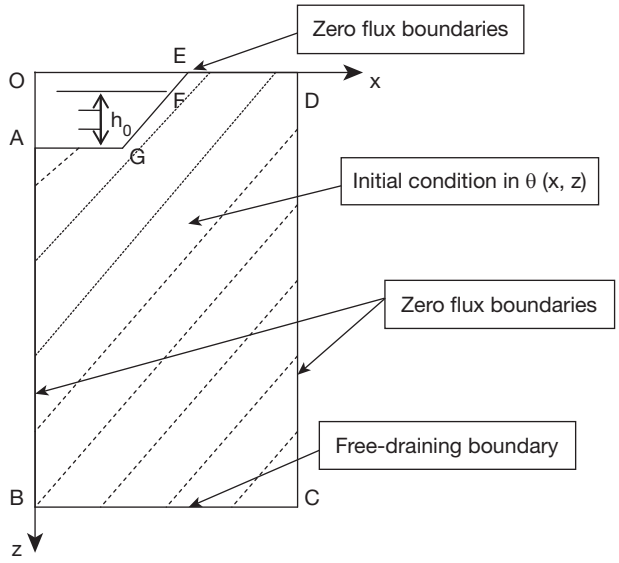

Fig. 2. Schematic representation of the initial and boundary conditions for an irrigation event.

Table 3. Estimated soil hydraulic parameters of the van Genuchten-Mualem model

Exp. no.	Soil texture	θ_r ($cm^3\ cm^{-3}$)	θ_s ($cm^3\ cm^{-3}$)	α (cm^{-1})	n (−)	l (−)	K_s ($cm\ min^{-1}$)
1	Silty clay loam	0.083	0.453	0.007	2.001	0.5	0.022
3	Silt loam	0.050	0.434	0.008	2.050	0.5	0.031
5	Sandy loam	0.041	0.528	0.033	2.143	0.5	0.154

$$\theta(h) = \begin{cases} \theta_r + \dfrac{\theta_s - \theta_r}{(1 + |\alpha h|^n)^m} & h < 0 \\ \theta_s & h \geq 0 \end{cases} \quad (3)$$

$$\theta_s = 1 - \frac{\rho_b}{\rho_s} \quad (4)$$

where

$$S_e = \frac{\theta - \theta_r}{\theta_s - \theta_r},\ m = 1 - \frac{1}{n},\ n > 1 \quad (5)$$

and θ_r is the residual soil water content ($cm^3\ cm^{-3}$), θ_s is the saturated soil water content ($cm^3\ cm^{-3}$), K_s is the saturated hydraulic conductivity ($cm\ min^{-1}$), m, n are empirical parameters related to the pore-size distribution, α is an empirical constant that is inversely related to the air-entry pressure value (min^{-1}), l is an empirical shape parameter, ρ_b is bulk density ($g\ cm^{-3}$), ρ_s is particle density (2.65 $g\ cm^{-3}$), and S_e is the effective saturation.

Initial and Boundary Conditions

We simulated a presumed two-dimensional (2D) symmetric vertical profile of the soil (Mailhol et al. 2007; Ebrahimian et al. 2011). Initial and boundary conditions for the simulation of cross-sectional ridge-furrow configuration are shown in Fig. 2. The simulated flow domain, for which the numerical solution was obtained, was 60 cm in width (BC section) and 90 cm in depth (DC section). The initial condition in the simulation was constant soil water content. During water application, the upper boundary condition along AGF was kept at a constant pressure head (h_0). A zero flux boundary condition was used on the soil surface ED, EF as evaporation could be neglected due to the plastic mulch covering. Zero flux boundary condition was applied to the middle of the furrow cross-section AB and ridge cross-section CD. Lateral water flux on both sides of the flow domain was zero (Zhang et al. 2005; Nie et al. 2009a). The bottom boundary (BC section) was simulated as free drainage. Information concerning implementation of these boundary conditions and numerical solution method can be found in the HYDRUS-2D user manual (Šimůnek et al. 2006).

Model Parameters Estimation

A pedotransfer function software package ROSETTA (Schaap et al. 2001) was used to provide the initial estimates of soil hydraulic parameters from soil particle size distribution and bulk density (Table 1). Saturated soil water content was calculated based on Eq. 4. The HYDRUS-2D simulations with the Rosetta-estimated parameters did not provide a good description of soil water dynamics during ridge-furrow infiltration. Due to the repacked soil used in the experiment, soil saturated hydraulic conductivity was likely affected by the soil structure. In Table 2, exps. 1, 3, and 5 were used to optimize soil hydraulic parameters of the van Genuchten–Mualem model in silty clay loam soil, silt loam soil, and sandy loam soil. Saturated hydraulic conductivity and parameter n were inversely estimated using HYDRUS-2D to get a better description of soil water movement (Šimůnek et al. 2006). Cumulative infiltration was used in the objective function during the optimization process. In Table 3, parameters θ_r and α were estimated by ROSETTA, θ_s was calculated against Eq. 4, parameters n and K_s were inversely estimated by HYDRUS-2D, and l was set as 0.5. The estimated soil hydraulic parameters were subsequently validated using the other experimental data. Experiments 2, 4, and 6 were conducted specifically for this purpose in silty clay loam soil, silt loam soil, and sandy loam soil (Table 2). Soil texture, initial soil moisture, furrow size and water depth used in HYDRUS-2D simulations are listed in Table 4 (Case 1–4).

Table 4. Soil texture, initial soil moisture, furrow size and water depth used in HYDRUS-2D simulations

Case	Soil texture	Initial soil moisture ($cm^3\ cm^{-3}$)	Wetted perimeter		Infiltration time (min)
			Furrow size (cm)	Furrow water depth (cm)	
1	Silty clay loam, Silt loam, Sandy loam	0.12	40	10	90
2	Silty clay loam	0.12, 0.18, 0.24	40	10	90
3	Silty clay loam	0.18	20, 40, 60	10	90
4	Silty clay loam	0.18	40	6, 10, 14	90

The geometry of experimental ridge-furrow configuration and furrow water depth was determined in order to infer geometry parameters required for the HYDRUS-2D numerical simulation. The simulation of soil water distribution, wetting pattern, and cumulative infiltration by HYDRUS-2D and the processing of data included the following steps: (1) setting water flow parameters including VG model and Mualem model; (2) creating simulated water flow domain geometry, nodes, and triangular elements; (3) setting the initial and boundary conditions; (4) running the HYDRUS-2D program. The nodes' soil water content values, wetting distance, and cumulative infiltration were used to validate the HYDRUS-2D model (Abbasi et al. 2004; Mailhol et al. 2007). We also prepared contour maps of the simulated soil water content using the SURFER code (Golden Software Version 8.0, 2002), using Kriging with a linear variogram.

Criterion for Model Evaluation

The performance indicators (RMSE, R^2) between simulated and observed values have commonly been used to evaluate the performance of the HYDRUS-2D model (Patel and Rajput 2008; Kandelous and Šimůnek 2010; Shan et al. 2011). RMSE was calculated as follows.

$$RMSE = \left[\frac{1}{n}\sum_{i=1}^{n}(I(o)_i - I(s)_i)^2\right]^{\frac{1}{2}} \quad (6)$$

where n is the total number of data in each experiment; $I(o)_i$ is the ith observed data; $I(s)_i$ is the ith simulated data. The statistical index R^2 for each simulation was automatically given using OriginLab 8.0 software (OriginLab Corporation, Northampton, USA). The RMSE and R^2 provide a quantitative comparison of the goodness-of-fit between simulated and observed cumulative infiltration.

RESULTS AND DISCUSSION

Soil Water Transport Model Calibration and Validation

Table 3 lists the soil hydraulic parameters that were obtained through simultaneous parameters estimation. Model calibrations were performed in exps. 1, 3, and 5 for silty clay loam soil, silt loam soil, and sandy loam soil, respectively. The observed and calibrated cumulative infiltration, soil water contents, and wetting distances for the three soil types were compared (Fig. 3). The R^2 values for cumulative infiltration, wetting distance, and soil water content were 0.987, 0.937, and 0.650, respectively. The lowest R^2 value for soil water content is caused by only cumulative infiltration as the objective function during model calibration. Also we believe that the van Genuchten–Mualem model from Eq. 4 overestimated parameter θ_s (Table 3). The laboratory-measured saturated soil water content is often much lower than the calculated value (Eq. 4)

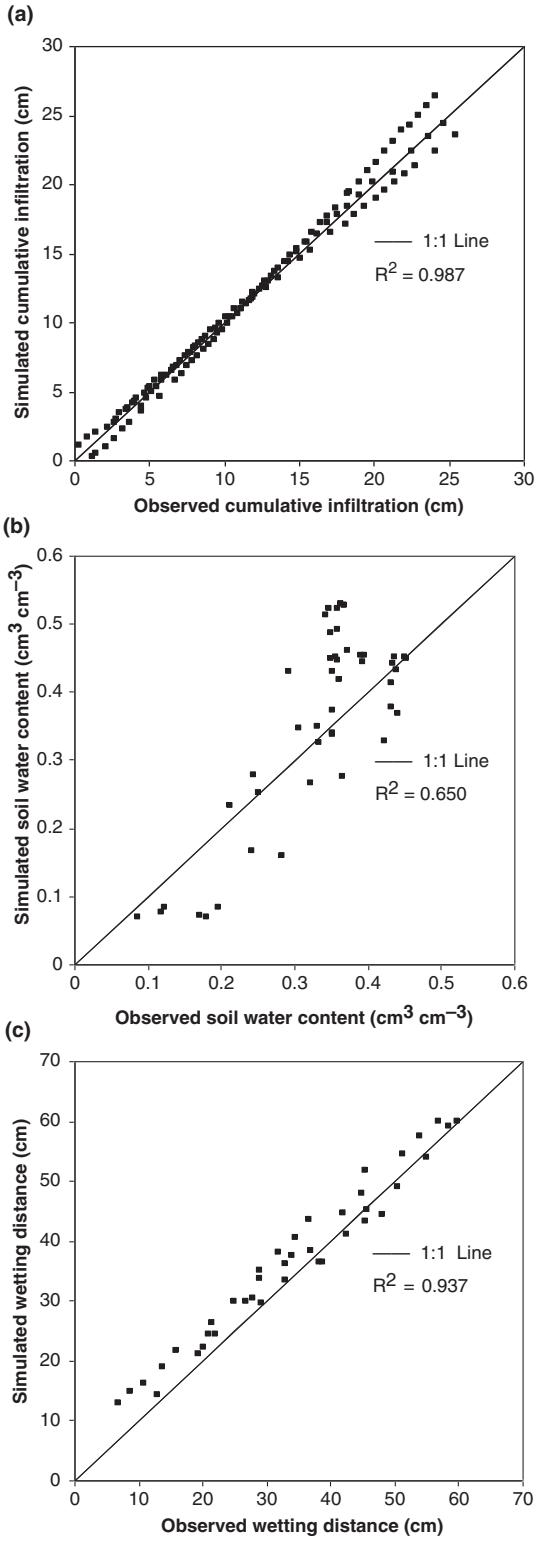

Fig. 3. Observed versus calibrated cumulative infiltration (a), soil water contents (b), wetting distances (c) for exps. 1, 3, and 5 in silty clay loam soil, silt loam soil, and sandy loam soil, respectively (R^2 values represent regression of observed versus corresponding calibrated data for exps. 1, 3, and 5).

Table 5. Statistical analysis for the comparison of observed and simulated cumulative infiltration

Measurement	Simulation process	Exp. no.	Soil texture	RMSE (cm)	R^2 (−)
Cumulative infiltration	Calibration	1	Silty clay loam	0.732	0.999
		3	Silt loam	1.416	0.974
		5	Sandy loam	0.991	0.981
	Validation	2	Silty clay loam	0.225	0.998
		4	Silt loam	0.438	0.995
		6	Sandy loam	0.206	0.994

because of entrapped or dissolved air in the sample (Abbasi et al. 2004). A statistical comparison between observed and simulated cumulative infiltration is presented in Table 5. The RMSE and R^2 values were satisfactory in silty clay loam soil, silt loam soil, and sandy loam soil. The obtained soil hydraulic parameters were reasonable compared with the common ranges reported in the literature (Šimůnek et al. 2006; Nie et al. 2009a).

The inversely estimated soil hydraulic parameters through the HYDRUS-2D model were validated using data from exps. 2, 4, and 6 in silty clay loam soil, silt loam soil, and sandy loam soil, respectively. The observed and predicted cumulative infiltration over time in three soil types is presented in Fig. 4. The HYDRUS-2D model with the estimated parameters effectively simulated cumulative infiltration during ridge-furrow infiltration. At furrow, ridge shoulder, and ridge locations, the observed and predicted soil water contents for the three different soil types were compared in Fig. 5. There were discrepancies between measured and simulated soil water contents at some positions of ridge-furrow geometry, and most of the observed soil water contents were lower than predicted values. No hysteresis of soil water characteristic curve was set in the simulations, which led to the discrepancy of observed and predicted water contents. The measured saturated soil water contents immediately after water supply were lower than the calculated values (Eq. 4) because of air entrapment, which may also contribute to the discrepancy in water contents. The larger discrepancy between predicted and observed soil water contents was also reported in other studies (Abbasi et al. 2004; Ebrahimian et al. 2011). Fig. 6 presents measured and predicted two-dimensional wetting distances in the silty clay loam soil, silt loam soil, and sandy loam soil, respectively. Note that the observed wetted horizontal and vertical distances were close to the predicted values. The values of RMSE were 0.225, 0.438, and 0.206, and R^2 values were 0.998, 0.995, and 0.994 for the three soil types, respectively (Table 5). These results confirm that the HYDRUS-2D model can be used to accurately simulate two-dimensional soil water movement in ridge-furrow irrigation system.

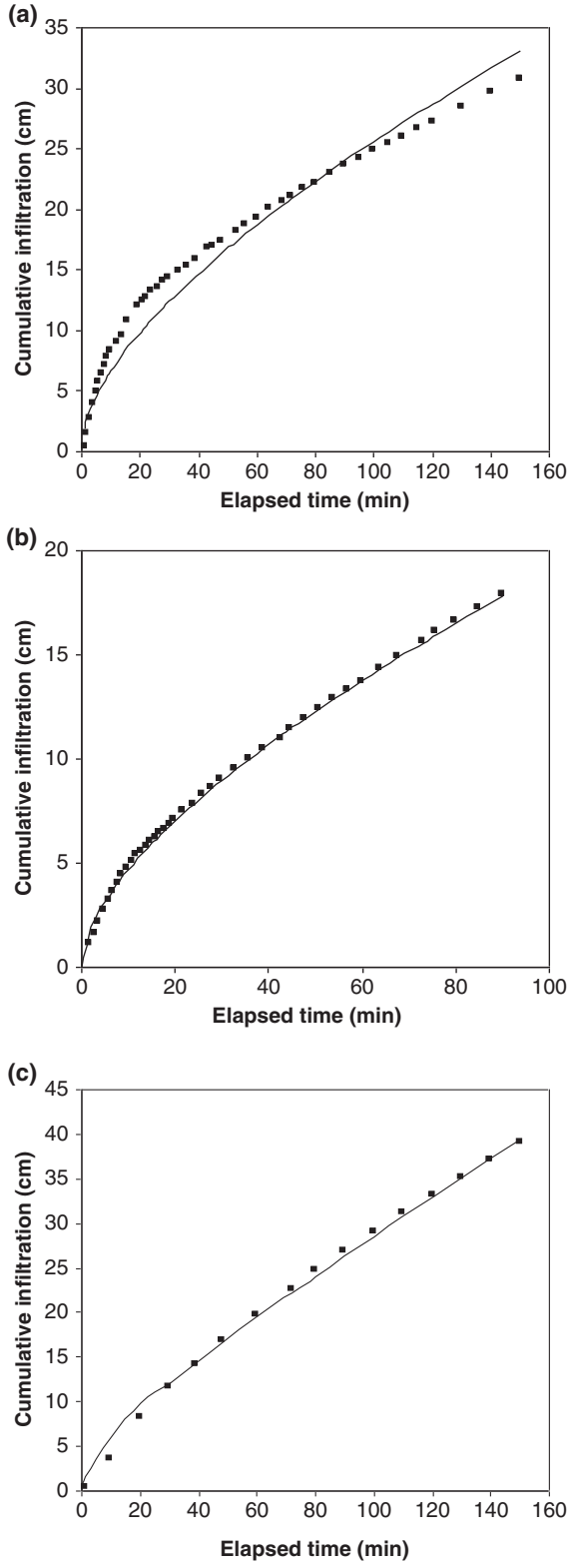

Fig. 4. Observed versus predicted cumulative infiltration for exps. 2, 4, and 6 in silty clay loam soil (a), silt loam soil (b), and sandy loam soil (c), respectively (observed: symbol, predicted: solid line).

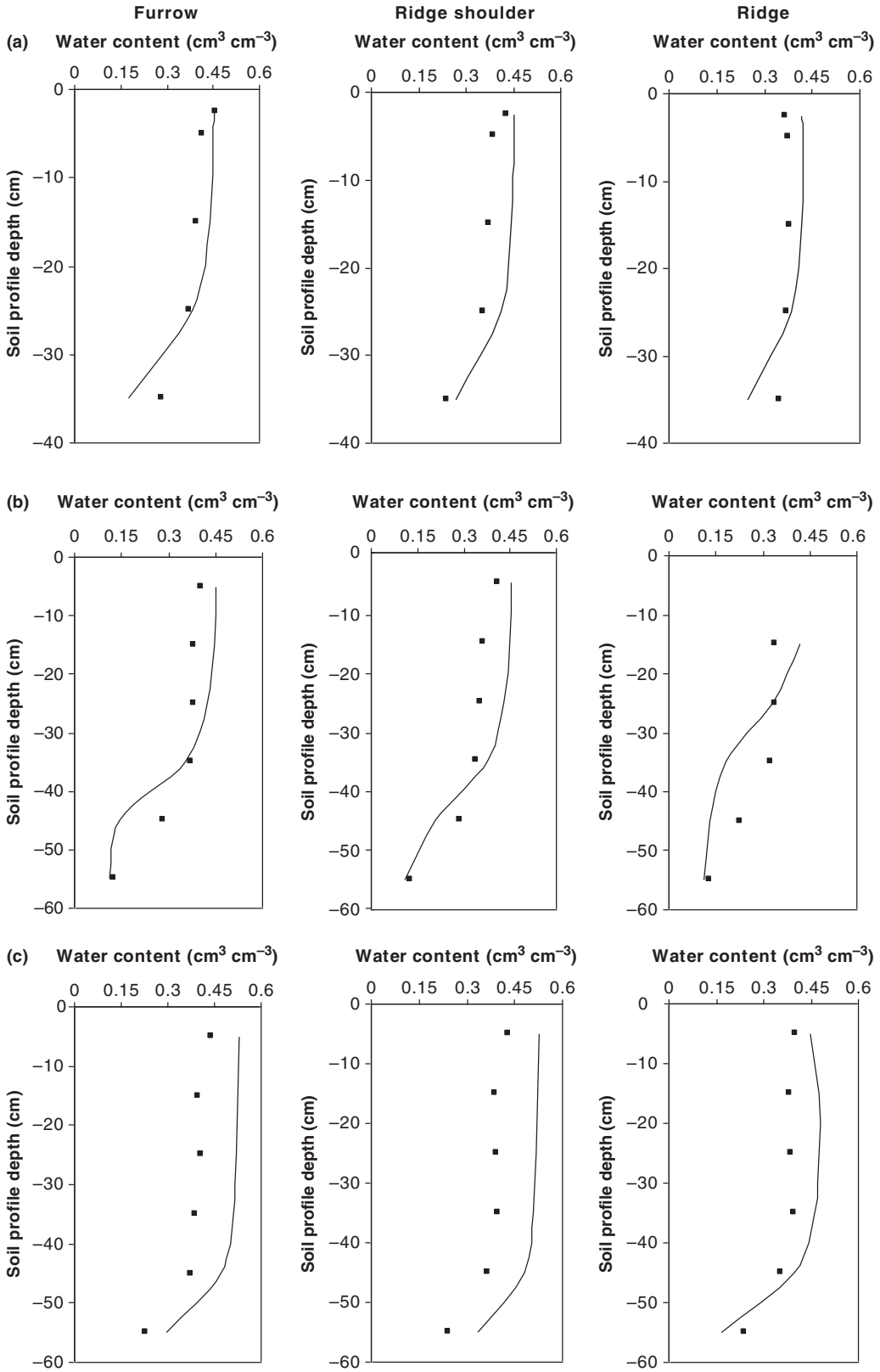

Fig. 5. Observed versus predicted soil water contents for furrow, ridge shoulder, and ridge positions of exps. 2, 4, and 6 in silty clay loam soil (a), silt loam soil (b), and sandy loam soil (c), respectively (observed: symbol, predicted: solid line).

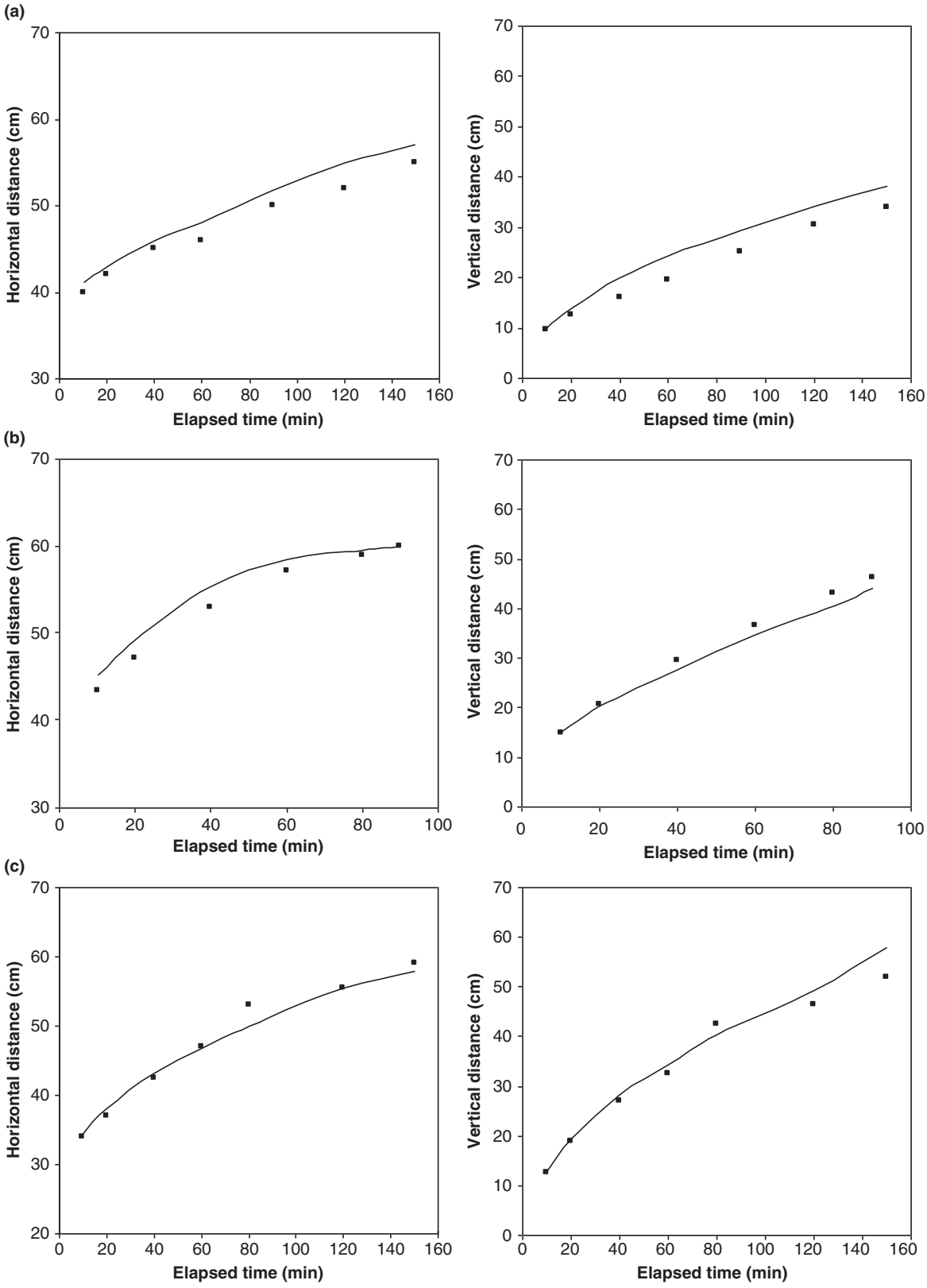

Fig. 6. Observed versus predicted two-dimensional wetting distances for exps. 2, 4, and 6 in silty clay loam soil (a), silt loam soil (b), and sandy loam soil (c), respectively (observed: symbol, predicted: solid line).

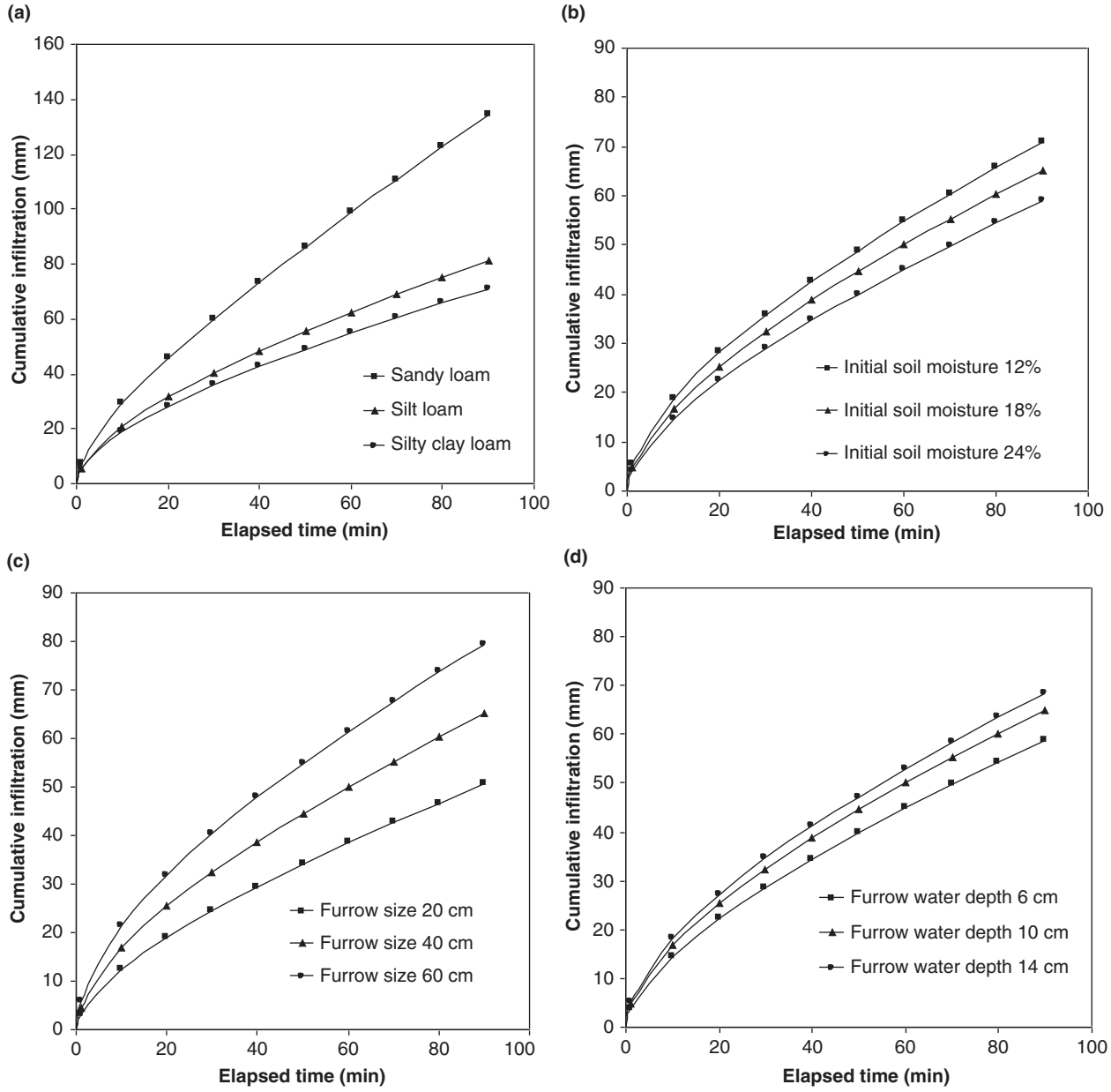

Fig. 7. Effect of variables on simulated cumulative infiltration in HYDRUS-2D simulations for Case 1 (a), 2 (b), 3 (c), and 4 (d), respectively.

Effects of Soil Texture, Initial Water Content, Furrow Size and Water depth on Cumulative Infiltration and Soil Water Distribution

Soil Texture

Cumulative infiltration and soil water distribution in the three soil types was simulated using the HYDRUS-2D model (Table 4, Case 1). Three categories of soil hydraulic parameters are given in Table 3. Figures 7a and 8a illustrate the effect of soil texture on cumulative infiltration and soil water distribution. The cumulative infiltration in 90 min was greatest in sandy loam soil (Fig. 7a) because of the higher total porosity (θ_s in Table 3) and likely more macropores. The volume of wetted soil was the greatest in sandy loam soil (Fig. 8a) because of greater saturated hydraulic conductivity (K_s in Table 3). The wetted vertical distance was greater than the wetted horizontal distance because of gravitational gradient in the vertical direction. Therefore, a high potential of deep water percolation can be expected in sandy loam soil under conditions of negligible evaporation and no plant water uptake. Water flow toward the ridges depends on capillary forces, which are relatively small in the coarse-textured sandy loam soil

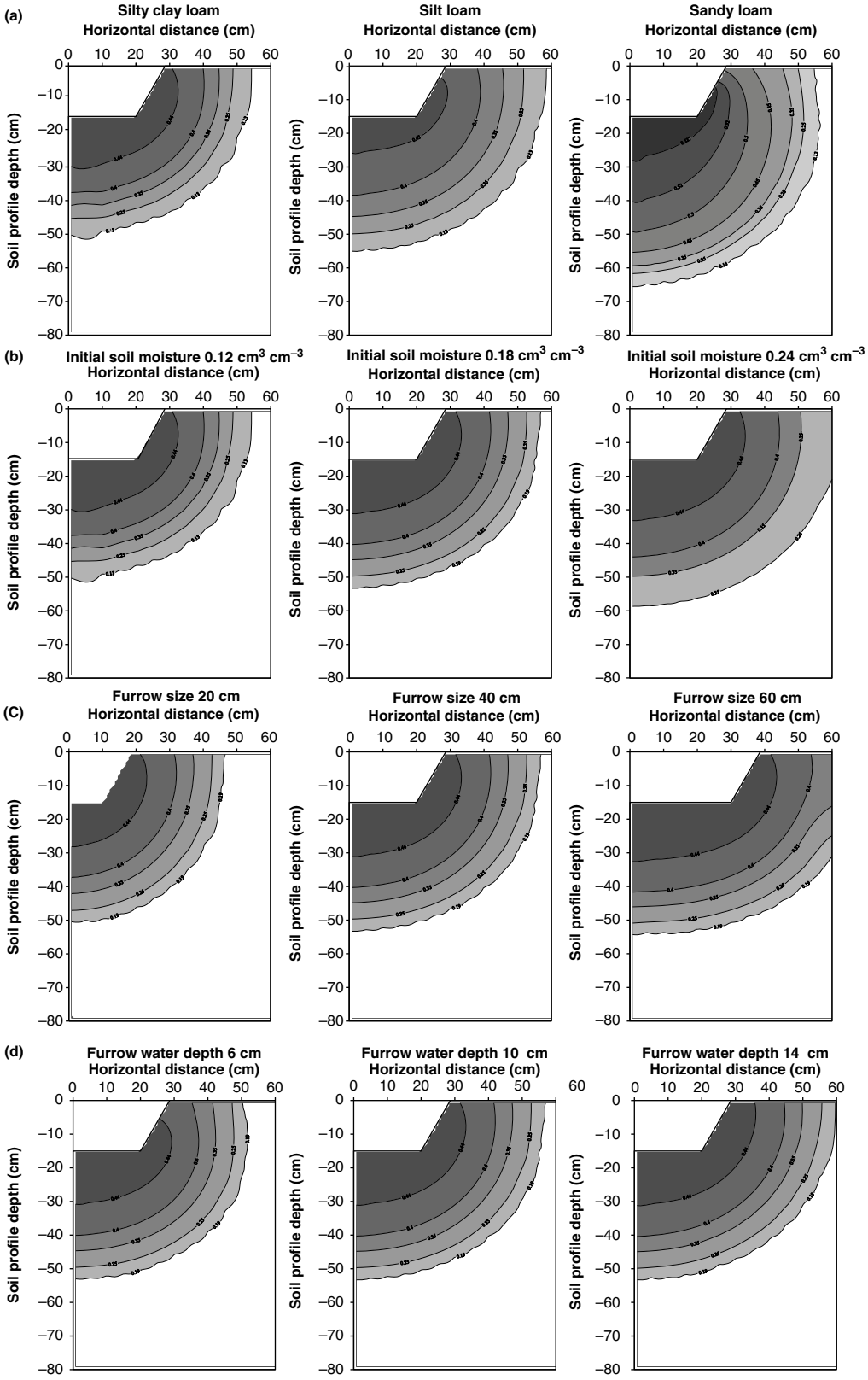

Fig. 8. Effect of variables on simulated soil water distribution in HYDRUS-2D simulations for Case 1 (a), 2 (b), 3 (c), and 4 (d), respectively.

(Abbasi et al. 2003b). The wetted distance of finer soils (silty clay loam and silt loam) was almost equal in vertical and horizontal directions, so the soil water distribution was more uniform in finer soils compared with coarser soil. Therefore, the wetted vertical distance could be determined according to the horizontal distance for the finer soils in field.

Initial Soil Water Content

The effect of initial soil water content on cumulative infiltration and soil water distribution (Table 4, Case 2) is illustrated in Figs. 7b and 8b. Cumulative infiltration in silty clay loam soil decreased with the increase in initial soil water content from 0.12 to 0.24 $cm^3\ cm^{-3}$ (Fig. 7b). A greater initial soil water content resulted in a lower soil matric potential gradient between the soil surface and soil at depth during water infiltration (Nie et al. 2009a). However, greater initial soil water content yielded larger wetted horizontal and downward distances (Fig. 8b). The unsaturated wetted zone can be easily saturated and the rate of advance of the wetting front was higher when initial soil water content was greater. Therefore, the irrigation schedule should be adjusted in a timely manner when soil water contents begin to affect crop development. The effect of initial soil water content should be considered as an independent parameter to develop a general infiltration model in ridge-furrow configuration.

Wetted Perimeter (Furrow Size and Furrow Water Depth)

The wetted perimeter affecting soil water dynamics was mainly due to furrow size and water depth in ridge-furrow infiltration. The effect of furrow size on cumulative infiltration and soil water distribution (Table 4, Case 3) is illustrated in Figs. 7c and 8c. It can be seen that wider furrow size resulted in greater cumulative infiltration (Fig. 7c). The wetting pattern was significantly different in the three furrow sizes (Fig. 8c). Lateral water flow and spreading were clear from furrows to ridges, which was illustrated by quasi one-dimensional water infiltration. It was caused by the greater surface infiltration area and water entry in saturated zone on furrow bed during the same infiltration duration. The vertical distances for the furrow size of 20 to 60 cm were almost equal. An increase in the surface infiltration area resulted in the increase of wetted horizontal distance, while the effect of surface flow area on the wetted soil depth was not significant (Khan et al. 1996; Li et al. 2003). Therefore, we should select narrow furrows for crops with deep rooting depth and wide furrows for crops with shallow rooting depth. In general, better irrigation uniformity in the 40-cm furrow size is recommended in ridge-furrow irrigation system.

Figures 7d and 8d show the influence of furrow water depth on cumulative infiltration and soil water distribution (Table 4, Case 4). The greater the water depth, the greater the wetted perimeter and gravitational potential on furrow bed, thus the more cumulative infiltration was produced (Fig. 7d). The volume of wetted soil for the 14-cm furrow water depth was larger than that of the 6-cm and 10-cm water depth, especially in the horizontal direction. In the stagnant blocked furrow, infiltration theory and previous studies showed that there is a positive correlation between cumulative infiltration and wetted perimeter in homogeneous soil (Sterlkoff and Sousa 1984; Izadi and Wallender 1985; Abbasi et al. 2003a). However, cumulative infiltration had a slightly negative relationship to wetted perimeter in non-homogeneous soil layers. Furthermore, the wetting patterns overlapped between adjacent furrows and likely decreased the effect of the wetted perimeter. Based on the foregoing analysis, irrigation with greater water depth produced more uniform water distribution throughout the root zone in the field, and also caused relatively less deep water percolation when compared with lower water depth.

In this study, the complexity caused by plant uptake, microclimate, and soil spatial variability was not considered. Further research on the effects of plant uptake and spatial variability on soil water infiltration is necessary in ridge-furrow irrigation system.

CONCLUSIONS

In this study, we validated the accuracy of HYDRUS-2D simulations of cumulative infiltration and soil water distribution in a ridge-furrow irrigation system. Three laboratory experiments in silty clay loam soil, silt loam soil, and sandy loam soil were conducted to calibrate and validate the HYDRUS-2D numerical code. Agreement between observed and predicted cumulative infiltration and wetting distances were satisfactory with the optimized parameters, whereas most of the observed soil water contents were lower than predicted values due to hysteresis and over-estimated parameter θ_s. The optimized parameters were accurate and the observed and simulated values were very close, which demonstrates that the HYDRUS-2D model can accurately simulate soil water dynamics and applied water volume under these conditions in ridge-furrow irrigation system.

This research also evaluated the effects of soil texture, initial soil water content, and wetted perimeter on soil water dynamics using HYDRUS-2D. Cumulative infiltration in sandy loam soil was greater, followed by the finer soil types (silt loam and silty clay loam). In finer soils, the wetted vertical and horizontal distances were equal and irrigation uniformity was better than in coarser soil. A high potential of deep water percolation was also produced in sandy loam soil. Cumulative infiltration decreased with the increase in initial soil water content, whereas the volume of wetted soil increased with the increase in initial soil water content. The effect of initial soil water content should be considered as a parameter to develop general infiltration models in ridge-furrow configuration. The wetted

perimeter affecting soil water dynamics was mainly due to furrow size and water depth. Both cumulative infiltration and the volume of wetted soil increased with the increase in wetter perimeter in a homogeneous soil. Narrow furrows for crops with deep rooting depth and wide furrows for crops with shallow rooting depth were selected in irrigation design. Irrigation with 40-cm furrow size and higher water depth are recommended in ridge-furrow irrigation system, while also producing better irrigation uniformity and relatively less deep water percolation throughout the root zone. The results obtained from the HYDRUS-2D model would be useful for the design, operation, and management of the ridge-furrow irrigation system.

ACKNOWLEDGEMENTS

This work is jointly supported by the Special Foundation of National Science & Technology Supporting Plan (2011BAD29B09), the "111" Project (B12007), and the Supporting Plan of Young Elites and the basic operational cost of research from Northwest A & F University. We are grateful to Fengyun Zhang, Qingling Geng, and Xiaoli Chen for their valuable suggestions on the manuscript, and Ping Li and Martin Parkers for the English language editing. We also would like to thank anonymous reviewers and the editors for the constructive comments on this manuscript.

Abbasi, F., Adamsen, F. J., Hunsaker, D. J., Feyen, J., Shouse, P. and van Genuchten, M. Th. 2003a. Effects of flow depth on water flow and solute transport in furrow irrigation: field data analysis. J. Irrig. Drainage Eng. ASCE **129**: 237–246.

Abbsai, F., Feyen, J., Roth, R. L., Sheedy, M. and van Genuchten, M. Th. 2003b. Water flow and solute transport in furrow-irrigated fields. Irrig. Sci. **22**: 57–65.

Abbsai, F., Feyen, J. and van Genuchten, M. Th. 2004. Two-dimensional simulation of water flow and solute transport below furrows: model calibration and validation. J. Hydrol. **290**: 63–79.

Crevoisier, D., Popova, Z., Mailhol, J. C. and Ruelle, P. 2008. Assessment and simulation of water and nitrogen transfer under furrow irrigation. Agric. Water Manage. **95**: 354–366.

Ebrahimian, H., Liaghat, A., Parsinejad, M., Playán, E., Abbasi, F. and Navabian, M. 2011. Simulation of 1D surface and 2D subsurface water flow and nitrate transport in alternate and conventional furrow fertigation. Irrig. Sci. doi: 10.1007/s00271-011-0303-3.

Esfandiari, M. and Maheshwari, B. L. 1997. Application of the optimization method for estimating infiltration characteristics in furrow irrigation and its comparison with other methods. Agric. Water Manage. **34**: 169–185.

Holzapfel, E. A., Jara, J., Zuñiga, C., Mariño, M. A., Paredes, J. and Billib, M. 2004. Infiltration parameters for furrow irrigation. Agric. Water Manage. **68**: 19–32.

Izadi, B. and Wallender, W. W. 1985. Furrow hydraulic characteristics and infiltration. Trans. ASABE **28**: 1901–1908.

Kandelous, M. M. and Šimůnek, J. 2010. Numerical simulations of water movement in as subsurface drip irrigation system under field and laboratory conditions using HYDRUS-2D. Agric. Water Manage. **97**: 1070–1076.

Khan, A. A., Yitayew, M. and Warrick, A. W. 1996. Field evaluation of water and solute distribution from a point source. J. Irrig. Drainage Eng. ASCE **122**: 221–227.

Li, J. S., Zhang, J. J. and Ren, L. 2003. Water and nitrogen distribution as affected by fertigation of ammonium nitrate from a point source. Irrig. Sci. **22**: 19–30.

Li, X. L., Su, D. R. and Yuan, Q. H. 2007. Ridge-furrow planting of alfalfa for improved rainwater harvest in rainfed semiarid areas in Northwest China. Soil Tillage Res. **93**: 117–125.

Li, X. Y. and Gong, J. D. 2002. Effects of different ridge: furrow ratios and supplemental irrigation on crop production in ridge and furrow rainfall harvesting system with mulches. Agric. Water Manage. **54**: 243–254.

Liu, T. R. and Lu, J. X. 1989. Studies on the cumulative infiltration of the two-dimensional infiltration under furrow irrigation. Journal of Hydraulic Engineering **4**: **11–21** [in Chinese with English abstract].

Liu, Y., Li, S. Q., Chen, F., Yang, S. J. and Chen, X. P. 2010. Soil water dynamics and water use efficiency in spring maize (*Zea mays* L.) fields subjected to different water management practices on the Loess Plateau, China. Agric. Water Manage. **97**: 769–775.

Mailhol, J. C., Crevoisier, D. and Triki, K. 2007. Impact of water application conditions on nitrogen leaching under furrow irrigation: experimental and modeling approaches. Agric. Water Manage. **87**: 275–284.

Moravejalahkami, B., Mostafazadeh-Fard, B., Heidarpour, M. and Abbasi, F. 2009. Furrow infiltration and roughness prediction for different furrow inflow hydrograph using a zero-inertia model with a multilevel calibration approach. Biosyst. Eng. **103**: 374–381.

Mualem, Y. 1976. A new model for predicting the hydraulic conductivity of unsaturated porous media. Water Resour. Res. **12**: 513–522.

Nie, W. B., Ma, X. Y. and Wang, S. L. 2009a. Infiltration model and numerical simulation of the soil water movement in furrow irrigation. Adv. Water Sci. **20**: 668–676 [in Chinese with English abstract].

Nie, W. B., Ma, X. Y. and Wang, S. L. 2009b. Forecast model for wetting front migration distance under furrow irrigation infiltration. Trans. CSAE **25**: 20–25 [in Chinese with English abstract].

Patel, N. and Rajput, T. B. S. 2008. Dynamics and modeling of soil water under subsurface drip irrigated onion. Agric. Water Manage. **95**: 1335–1349.

Richards, L. A. 1931. Capillary conduction of liquids through porous mediums. Physics **1**: 318–333.

Schaap, M. G., Leij, F. J. and van Genuchten, M. Th. 2001. ROSETTA: a computer program for estimating soil hydraulic properties with hierarchical pedotransfer functions. J. Hydrol. **251**: 163–176.

Shan, Y. Y., Wang, Q. J. and Wang, C. X. 2011. Simulated and measured soil wetting patterns for overlap zone under double points sources of drip irrigation. Afr. J. Biotechnol. **10**: 13744–13755.

Šimůnek, J., van Genuchten, M. Th. and Šejna, M. 2006. The HYDRUS software package for simulating the two- and three-dimensional movement of water, heat, and multiple solutes in variably saturated media. Technical Manual, Version 1.0. PC progress, Prague, Czech Republic.

Skaggs, T. H., Trout, T. J., Šimůnek, J. and Shouse, P. J. 2004. Comparison of HYDRUS-2D simulations of drip

irrigation with experimental observations. J. Irrig. Drainage Eng. ASCE **130**: 304–310.

Strelkoff, T. and Souza, F. 1984. Modeling effect of depth on furrow infiltration. J. Irrig. Drainage Eng. ASCE **110**: 375–387.

Sun, X. H., Wang, W. Y. and Dang, Z. L. 1994. Testing study of the effects of infiltration parameters in furrow irrigation. Journal of Northwest A & F University **22**: 102–106 [in Chinese with English abstract].

Tabuada, M. A., Rego, Z. J. C., Vachaud, G. and Pereira, L. S. 1995. Two-dimensional infiltration under furrow irrigation: Modeling, its validation and application. Agric. Water Manage. **27**: 105–123.

Trout, T. J. 1992. Flow velocity and wetted perimeter effects on furrow infiltration. Trans. ASABE **35**: 855–863.

van Genuchten, M. Th. 1980. A closed-form equation for predicting the hydraulic conductivity of unsaturated soils. Soil Sci. Soc. Am. J. **44**: 892–898.

Wang, D., Yates, S. R., Simunek, J. and van Genuchten, M. Th. 1997. Solute transport in simulated conductivity fields under different irrigations. J. Irrig. Drainage Eng. ASCE **123**: 336–343.

Yao, W. W., Ma, X. Y., Li, J. and Parks, M. 2010. Simulation of point source wetting pattern of subsurface drip irrigation. Irrig. Sci. **29**: 331–339.

Zhang, X. Y., Cai, H. J. and Wang, J. 2005. Experimental study on influence factors of two-dimensional infiltration in furrow irrigation. Trans. CASE **21**: 38–41 [in Chinese with English abstract].